

# Design of Bayesian Clinical Trials with Clustered Data and Multiple Endpoints

Luke Hagar\*      Shirin Golchi

*Department of Epidemiology, Biostatistics & Occupational Health, McGill University*

## Abstract

In the design of clinical trials, it is essential to assess the design operating characteristics (i.e., the probabilities of making correct decisions). Common practice for the evaluation of operating characteristics in Bayesian clinical trials relies on estimating the sampling distribution of posterior summaries via Monte Carlo simulation. It is computationally intensive to repeat this estimation process for each design configuration considered, particularly for clustered data that are analyzed using complex, high-dimensional models. In this paper, we propose an efficient method to assess operating characteristics and determine sample sizes for Bayesian trials with clustered data and multiple endpoints. We prove theoretical results that enable posterior probabilities to be modelled as a function of the sample size. Using these functions, we assess operating characteristics at a range of sample sizes given simulations conducted at only two sample sizes. These theoretical results are also leveraged to quantify the impact of simulation variability on our sample size recommendations. The applicability of our methodology is illustrated using a current clinical trial with clustered data.

**Keywords:** Cluster randomized trials; experimental design; longitudinal studies; marginal estimands; posterior probabilities; sample size determination

## 1 Introduction

Bayesian methods for data-driven decision making have become increasingly popular in the design and analysis of clinical trials. Decision making in Bayesian clinical trials is often based on posterior and posterior predictive probabilities (Spiegelhalter et al., 2004; Berry et al., 2010). In many cases, despite the use of Bayesian analysis and decision criteria, grant and regulatory agencies require the design to be assessed with respect to frequentist operating characteristics (FDA, 2019). Certain operating characteristics, such as power and the type I error rate, are considered for most Bayesian trials. Additional operating characteristics including the probabilities of making certain interim decisions are also of interest in adaptive designs. In Bayesian trials, sampling distributions of posterior summaries must be accurately estimated to correctly assess the frequentist operating characteristics. Sample size determination (SSD) procedures rely on accurate estimates of these operating characteristics.

Wang and Gelfand (2002) proposed a general framework for Bayesian SSD in which Monte Carlo simulation is used to accurately estimate frequentist operating characteristics of Bayesian designs. This computational approach estimates sampling distributions by simulating many repetitions of a trial with a particular

---

\*Luke Hagar is the corresponding author and may be contacted at [luke.hagar@mail.mcgill.ca](mailto:luke.hagar@mail.mcgill.ca).

set of design, analysis, and decision parameters. In comprehensive trial design, these numerical studies can involve many scenarios, each of which is defined by a different combination of design, analysis, and decision parameters. Design parameters may include sample sizes in adaptive and non-adaptive contexts; analysis parameters may include the effect size for the estimand of interest and values for nuisance parameters; and decision parameters may include thresholds for efficacy or futility. These simulations often borrow from the frequentist framework for power analysis in that each scenario and its corresponding sampling distribution are defined given fixed choices for the design, analysis, and decision parameters. Alternative Bayesian SSD approaches in which sampling distributions of posterior summaries are marginalized with respect to a *design prior* that incorporates uncertainty in the model parameters have also been proposed (O’Hagan et al., 2005; De Santis, 2007; Gubbiotti and De Santis, 2011).

The U.S. Food and Drug Administration (FDA) recommends using at least  $10^4$  simulation repetitions to estimate the sampling distribution for each scenario considered (FDA, 2019). Each simulation repetition for each scenario typically involves computational posterior approximation. The computational burden associated with posterior approximation is substantial for high-dimensional models, including those for clustered data that use random effects to model within-cluster dependence. Clustered data are common in clinical settings (e.g., longitudinal studies and cluster randomized trials). In trials where generalized linear models are employed for analysis, further computing resources are required to construct marginal estimands via Bayesian G-computation (Kalton, 1968; Keil et al., 2018; Daniel et al., 2021; Willard et al., 2024). These estimands are obtained by marginalizing samples from the posterior distribution with respect to the distribution of additional covariates or random effects. Drawing inference based on *marginal* estimands is important when population average treatment effects are of interest but adjusted analyses are employed (Willard et al., 2024).

Moreover, many modern designs leverage co-primary or secondary outcomes in decision making, resulting in complex decision criteria. Each of these endpoints addresses a distinct aspect of a disease, and it may be necessary to show the treatment provides clinical benefit across all or certain combinations of the outcomes (FDA, 2022). The literature on multiple endpoints in clinical trials primarily focuses on correcting for multiplicity in traditional designs (see e.g., Holm (1979); Dmitrienko et al. (2008); Bretz et al. (2009)), with minimal consideration of Bayesian approaches. In Bayesian trials with multiple endpoints, one must approximate multiple posterior distributions per simulation repetition or a more complicated posterior that jointly models all outcomes of interest. Because each simulation repetition expends valuable computing resources, it is important to develop methodology that ensures these numerical studies efficiently inform operating characteristic assessment and Bayesian SSD. Streamlined design methods reduce costs associated with trial design and enhance timely communication between the stakeholders of a clinical trial.

Various strategies have recently been proposed to reduce the computational burden associated with

estimating operating characteristics for Bayesian designs. [Han et al. \(2024\)](#) used optimization techniques to select a parsimonious set of simulation scenarios at which to conduct sensitivity analysis on the operating characteristics. [Golchi \(2022\)](#) proposed a modelling approach to estimate sampling distributions of posterior summaries and trial design operating characteristics using Gaussian processes; [Golchi and Willard \(2024\)](#) presented an alternative modelling method that augmented simulations with asymptotic theory. [Hagar and Stevens \(2024\)](#) approximated power curves using segments of the relevant sampling distributions. For a given simulation scenario, [Hagar and Stevens \(2025\)](#) proposed a method to assess operating characteristics across the sample size space using estimates of the sampling distribution at only two sample sizes. However, all existing work focuses on a single endpoint informed by independent observations. Since decisions in many trials are based on multiple estimands for dependent data, we build upon the method from [Hagar and Stevens \(2025\)](#) to facilitate the efficient assessment of operating characteristics in designs with clustered data and complex decision rules. Our proposed methods are simple to implement and promote an economical framework for simulation-based Bayesian SSD that is suitable for broad use with clinical trials.

The remainder of this article is structured as follows. In [Section 2](#), we introduce notation and prove new theoretical results about a proxy to the sampling distribution of posterior probabilities based on clustered data. In [Section 3](#), we adapt these theoretical results to develop a procedure for Bayesian SSD that requires estimation of the sampling distribution of posterior probabilities at only two sample sizes. This procedure also allows users to efficiently quantify the impact of simulation variability on the sample size recommendation. [Section 4](#) presents a Bayesian adaptive trial where households are randomized to preventative tuberculosis treatments and interim decisions are based on two secondary outcomes and a primary safety endpoint. The interim analysis for this trial serves to motivate our methodology and illustrate the application of our SSD approach. We conclude with a summary and discussion of extensions to this work in [Section 5](#).

## 2 Methodology

### 2.1 Operating Characteristics with Multiple Estimands

Consider a clinical trial where multiple outcomes related to treatment efficacy and safety must be evaluated. Each of these  $K \geq 1$  outcomes is summarized by a scalar estimand, giving rise to a vector of  $K$  estimands. Decisions in Bayesian trials are made using predefined decision rules based on posterior summaries of the estimands ([Berry et al., 2010](#)). This paper focuses on trials where decision criteria are defined with respect to posterior probabilities. The statistical model for the trial is defined using a set of parameters  $\boldsymbol{\theta} \in \Theta$ . The estimands are a function of these parameters:  $\boldsymbol{\delta}(\boldsymbol{\theta}) \in \mathbb{R}^K$ . The hypotheses that inform decision making are formulated as

$$H_0 : \boldsymbol{\delta}(\boldsymbol{\theta}) \notin (\boldsymbol{\delta}_L, \boldsymbol{\delta}_U) \quad \text{vs.} \quad H_1 : \boldsymbol{\delta}(\boldsymbol{\theta}) \in (\boldsymbol{\delta}_L, \boldsymbol{\delta}_U), \quad (1)$$

where  $\delta_L$  and  $\delta_U$  represent vectors of  $K$  interval endpoints. This general notation for  $\delta_L$  and  $\delta_U$  accommodates hypothesis tests based on superiority, noninferiority, and practical equivalence (Spiegelhalter et al., 1994, 2004). The  $k^{\text{th}}$  row of (1) outlines complementary hypotheses for the scalar estimand  $\delta_k(\boldsymbol{\theta})$ , defined as  $H_{0,k} : \delta_k(\boldsymbol{\theta}) \notin (\delta_{L,k}, \delta_{U,k})$  vs.  $H_{1,k} : \delta_k(\boldsymbol{\theta}) \in (\delta_{L,k}, \delta_{U,k})$ . Using this notation,  $H_1$  is true if and only if *all* subhypotheses  $\{H_{1,k}\}_{k=1}^K$  are true. Otherwise,  $H_0$  is true.

Multi-component decision criteria are defined using combinations of posterior probabilities about the individual estimands  $\{\delta_k(\boldsymbol{\theta})\}_{k=1}^K$  in  $\boldsymbol{\delta}(\boldsymbol{\theta})$ . The posterior of  $\boldsymbol{\theta}$  synthesizes information from the prior distribution for  $\boldsymbol{\theta}$  and the data  $\mathcal{D}_c$ . Since this paper focuses on clustered data,  $\mathcal{D}_c$  consists of  $N$  observations from clusters  $j = 1, \dots, c$ . There are  $n_j$  observations from cluster  $j$  such that  $\sum_{j=1}^c n_j = N$ . As described later, we index the data  $\mathcal{D}_c$  and consider SSD in terms of the number of clusters  $c$ . This framework accommodates various contexts where clustered data arise. In cluster randomized trials, individual observations correspond to distinct participants that are randomized to a given treatment in groups or clusters (Murray, 1998). Cluster randomized trials are practical in many real world settings and reduce the risk of contamination between treatment groups (Hemming et al., 2021). In longitudinal studies, individual observations correspond to repeated measurements from the same participant.

The data  $\mathcal{D}_c = \{\mathbf{Y}_{N \times K}, \mathbf{A}_N, \mathbf{X}_{N \times p}\}$  may consist of observed outcomes for each estimand  $\mathbf{Y}_{N \times K}$ , treatment assignments  $\mathbf{A}_N$ , and  $p$  additional covariates  $\mathbf{X}_{N \times p}$ . While we use this general notation, certain outcomes may not be related to all  $p$  additional covariates. These data are used to compute a vector of  $K$  posterior probabilities regarding the subhypotheses  $\{H_{1,k}\}_{k=1}^K$ :

$$\boldsymbol{\tau}(\mathcal{D}_c) = \begin{bmatrix} \tau_1(\mathcal{D}_c) \\ \tau_2(\mathcal{D}_c) \\ \vdots \\ \tau_K(\mathcal{D}_c) \end{bmatrix} = \begin{bmatrix} Pr(H_{1,1} | \mathcal{D}_c) \\ Pr(H_{1,2} | \mathcal{D}_c) \\ \vdots \\ Pr(H_{1,K} | \mathcal{D}_c) \end{bmatrix}. \quad (2)$$

Decision rules are defined by comparing  $\boldsymbol{\tau}(\mathcal{D}_c)$  to decision thresholds  $\boldsymbol{\gamma} \in [0, 1]^K$ . Depending on the context, the decision threshold  $\boldsymbol{\gamma}$  could guide conclusions about treatment superiority or futility. Complex decision rules in clinical trials may be constructed by considering any subset of the  $K$  individual comparisons between  $\boldsymbol{\tau}(\mathcal{D}_c)$  and  $\boldsymbol{\gamma}$ . To accommodate a broad range of decision rules, we define the binary indicator  $\nu(\mathcal{D}_c)$  that equals 1 if and only if the decision criteria are met when comparing  $\boldsymbol{\tau}(\mathcal{D}_c)$  with  $\boldsymbol{\gamma}$ .

When decision rules depend on  $K > 1$  estimands, we must consider the *joint* sampling distribution of the posterior probabilities in  $\boldsymbol{\tau}(\mathcal{D}_c)$  to estimate design operating characteristics. To assess sampling distributions of posterior probabilities via simulation, we define various data generation processes for  $\mathcal{D}_c$ . For each simulation repetition, data are generated according to a fixed parameter value  $\boldsymbol{\theta}$ . Additional parameters are required to generate the cluster sizes  $\{n_j\}_{j=1}^c$ , covariates  $\mathbf{X}_{N \times p}$ , and potential latent effects  $\mathbf{W}_{c \times q}$ ; we expand upon this discussion in Section 2.2. The probability model  $\Psi$  characterizes how  $\boldsymbol{\theta}$  values are drawn in each simulation repetition  $r = 1, \dots, m$ . The probability model  $\Psi$  could be viewed as a *design*

prior (De Santis, 2007; Berry et al., 2010; Gubbiotti and De Santis, 2011) that differs from the *analysis* prior  $p(\boldsymbol{\theta})$ . It is standard practice to estimate the sampling distribution of  $\boldsymbol{\tau}(\mathcal{D}_c)$  under  $\Psi$  as follows (Wang and Gelfand, 2002; Berry et al., 2010). For each simulation repetition  $r$ , data  $\mathcal{D}_{c,r}$  are generated given  $\boldsymbol{\theta}_r \sim \Psi$ , and  $\boldsymbol{\tau}(\mathcal{D}_{c,r})$  is computed. Across  $m$  simulation repetitions, the collection of obtained  $\{\boldsymbol{\tau}(\mathcal{D}_{c,r})\}_{r=1}^m$  values estimates the joint sampling distribution of  $\boldsymbol{\tau}(\mathcal{D}_c)$ .

We now define general operating characteristics with respect to the model from which  $\boldsymbol{\theta}$  values are drawn. For a given model  $\Psi$ , the probability of meeting all decision criteria is

$$\mathbb{E}_{\Psi}[Pr(\nu(\mathcal{D}_c) = 1 \mid \boldsymbol{\theta})] = \int Pr(\nu(\mathcal{D}_c) = 1 \mid \boldsymbol{\theta})\Psi(\boldsymbol{\theta})d\boldsymbol{\theta}. \quad (3)$$

Given our simulation results, the probability in (3) is estimated as

$$\frac{1}{m} \sum_{r=1}^m \mathbb{I}\{\nu(\mathcal{D}_{c,r}) = 1\}, \quad (4)$$

where  $\mathcal{D}_{c,r}$  are generated using  $\boldsymbol{\theta}_r$  obtained via  $\Psi$ . If  $H_1$  is true, we want the decision criteria to be satisfied. The probability of making the correct decision based on the data is  $\mathbb{E}_{\Psi_1}[Pr(\nu(\mathcal{D}_c) = 1 \mid \boldsymbol{\theta})]$  where  $\Psi_1$  is a probability model such that  $H_1$  is true. This probability is estimated using (4) when  $\mathcal{D}_{c,r}$  are generated using  $\boldsymbol{\theta}_r$  obtained via  $\Psi_1$ . In standard contexts where  $\boldsymbol{\gamma}$  is a vector of superiority thresholds, the probability of making the correct decision given a set of parameter values resulting from a degenerate  $\Psi_1$  is referred to as power. The term assurance is commonly used if  $\Psi_1$  incorporates uncertainty about the parametric assumptions used to generate the data (O'Hagan and Stevens, 2001). If  $H_0$  is instead true, we do *not* want the decision criteria to be satisfied. The probability of making the incorrect decision is defined as  $\mathbb{E}_{\Psi_0}[Pr(\nu(\mathcal{D}_c) = 1 \mid \boldsymbol{\theta})]$  where  $\Psi_0$  is a probability model such that  $H_0$  is true. Using  $\Psi_0$  instead of  $\Psi_1$ , this probability can be estimated as in (4). The probability of making the incorrect decision is the expected type I error rate in standard contexts where  $\boldsymbol{\gamma}$  represents superiority thresholds.

The decision thresholds  $\boldsymbol{\gamma}$  bound the probability of making the incorrect decision in a trial, and the choice for  $\boldsymbol{\gamma}$  is complicated by considering multiple estimands. The sample size  $c$  is selected to ensure the trial has a large enough probability of making the correct decision. For every value of  $c$  considered, we must obtain a collection of  $\{\boldsymbol{\tau}(\mathcal{D}_{c,r})\}_{r=1}^m$  values via simulation to estimate this probability in (4). The process to obtain the  $\{\boldsymbol{\tau}(\mathcal{D}_{c,r})\}_{r=1}^m$  values is often computationally intensive. However, we could reduce the computational burden by using previously estimated sampling distributions of  $\boldsymbol{\tau}(\mathcal{D}_c)$  to estimate operating characteristics at new  $c$  values. We could use this process to conduct SSD for Bayesian trials with substantially fewer simulation repetitions. We propose such a method for trial design in this paper and begin its development after a brief discussion of marginal estimands in Section 2.2

## 2.2 Marginal Estimands

The marginal estimands  $\delta(\boldsymbol{\theta})$  can be expressed as a contrast of population quantities for each treatment. We let  $A_i \in \{0, 1\}$  denote the treatment assignment associated with the  $i^{\text{th}}$  observation, where  $A_i = 1$  and  $A_i = 0$  respectively represent being randomized to the treatment and control groups. We let  $\boldsymbol{\mu}(\boldsymbol{\theta}; A)$  be the marginal mean corresponding to the treatment group  $A$ . We represent the marginal estimands by

$$\delta(\boldsymbol{\theta}) = \boldsymbol{\mu}(\boldsymbol{\theta}; A = 1) - \boldsymbol{\mu}(\boldsymbol{\theta}; A = 0), \quad (5)$$

where we use a difference-based contrast without loss of generality. For clustered data,  $Kq$  unobserved latent effects  $\mathbf{W}_{c \times Kq}$  account for the dependence between outcomes from the same cluster, where there are  $q$  latent effects for each of the  $K$  outcomes. We assume that these latent effects are not shared between observations from different clusters. As a result, we make the standard assumption that outcomes in different clusters are independent. The joint posterior of  $\boldsymbol{\theta}, \mathbf{W} \mid \mathcal{D}_c$  generally depends on  $p$  observed covariates  $\mathbf{X}_{N \times p}$ . Thus,  $\boldsymbol{\theta}$  may contain regression coefficients corresponding to the observed covariates and distributional parameters for the latent effects.

Samples from the posterior of  $\boldsymbol{\theta}, \mathbf{W} \mid \mathcal{D}_c$  give rise to posterior samples from the conditional parameter  $\boldsymbol{\mu}(\boldsymbol{\theta}; A, \mathbf{X}, \mathbf{W})$  with respect to fixed patterns for the covariates  $\mathbf{X}$  and latent effects  $\mathbf{W}$ . Because the estimands in clinical trials are often non-collapsible (Daniel et al., 2021; Willard et al., 2024), we marginalize the posterior samples of  $\boldsymbol{\mu}(\boldsymbol{\theta}; A, \mathbf{X}, \mathbf{W})$  with respect to the distributions of  $\mathbf{X}$  and  $\mathbf{W}$  to obtain samples from the posterior of

$$\boldsymbol{\mu}(\boldsymbol{\theta}; A) = \int_{\mathbf{X}} \int_{\mathbf{W}} \boldsymbol{\mu}(\boldsymbol{\theta}; A, \mathbf{X}, \mathbf{W}) p(\mathbf{X}) p(\mathbf{W}) d\mathbf{W} d\mathbf{X}.$$

The procedure to implement this marginalization is based on reweighting according to repeated sampling from Dirichlet distributions; its details are described in Web Appendix B. We use this procedure to approximate the posterior distribution of  $\delta(\boldsymbol{\theta})$ .

Lastly, we underscore why our methodology provides the option to marginalize over the distribution of the latent effects  $\mathbf{W}$ . Most cluster-specific models are predicated on the existence of latent risk groups that are indexed by the cluster-specific effects (Neuhaus et al., 1991). These latent risk groups may not be balanced for all treatment groups in trials with clustered data, impacting the validity of the trial’s conclusions. Since these cluster-specific effects are not observed, it is difficult to determine whether they are balanced between treatment groups. We therefore conduct inference by treating  $\mathbf{W}$  as additional variables that we marginalize over.

## 2.3 A Proxy to the Joint Sampling Distribution

To motivate our SSD procedure proposed in Section 3, we create a proxy to the joint sampling distribution of  $\boldsymbol{\tau}(\mathcal{D}_c)$ . These proxies are needed for the theory that underpins our proposed methodology. However,

our methods do not directly use these proxies and instead estimate true sampling distributions of  $\boldsymbol{\tau}(\mathcal{D}_c)$  by simulating samples  $\{\mathcal{D}_{c,r}\}_{r=1}^m$  and approximating posterior probabilities as described in Section 2.1. Our proxies are predicated on an asymptotic approximation to the posterior of  $\boldsymbol{\delta}(\boldsymbol{\theta})$  based on the Bernstein-von Mises (BvM) theorem (van der Vaart, 1998) that is detailed in Lemma 1.

We require that the four conditions for the BvM theorem are satisfied to apply our methodology. The first assumption is an independently and identically distributed assumption. We require that independence assumptions are satisfied at the cluster level but not at the observation level. The next two conditions concern the likelihood function and are weaker than the regularity conditions for the asymptotic normality of the maximum likelihood estimator (MLE) (Lehmann and Casella, 1998). For reasons described shortly, our methodology also requires that those regularity conditions are satisfied. The final condition for the BvM theorem concerns the analysis prior  $p(\boldsymbol{\theta})$ . This prior must be absolutely continuous with positive density in a neighbourhood of the true value for  $\boldsymbol{\theta}$ . For simulation repetition  $r$ , this true value of  $\boldsymbol{\theta}_r \sim \Psi$  is incorporated into Lemma 1.

**Lemma 1.** *Assume the conditions described above are satisfied for  $\boldsymbol{\theta}_r \sim \Psi$ . Let  $\hat{\boldsymbol{\delta}}_r^{(c)} = \boldsymbol{\delta}(\hat{\boldsymbol{\theta}}_r^{(c)})$  be the maximum likelihood estimate for  $\boldsymbol{\delta}(\boldsymbol{\theta})$  expressed in terms of the number of independent clusters  $c$ . As  $c$  increases, a large-sample approximation to the posterior of  $\boldsymbol{\delta}(\boldsymbol{\theta})$  takes the form*

$$\mathcal{N}\left(\hat{\boldsymbol{\delta}}_r^{(c)}, c^{-1}\boldsymbol{\Lambda}(\boldsymbol{\theta}_r)\right), \quad (6)$$

where  $\boldsymbol{\Lambda}(\boldsymbol{\theta}_r)$  is related to the Fisher information matrix  $\mathcal{I}(\boldsymbol{\theta})$ .

In Web Appendix A.1, we prove Lemma 1 and specify the form of the matrix  $\boldsymbol{\Lambda}(\boldsymbol{\theta}_r)$ . We also carefully justify that Lemma 1 holds true for marginal estimands as defined in (5) when the cluster sizes  $\{n_j\}_{j=1}^c$  are drawn according to a given probability distribution. Here, we use the approximation in (6) for theoretical development. The theory in Web Appendix A additionally demonstrates that the approximate sampling distribution of the MLE  $\hat{\boldsymbol{\delta}}^{(c)} \mid \boldsymbol{\theta} = \boldsymbol{\theta}_r$  is  $\mathcal{N}(\boldsymbol{\delta}_r, c^{-1}\boldsymbol{\Lambda}(\boldsymbol{\theta}_r))$  under the regularity conditions in Lehmann and Casella (1998), where  $\boldsymbol{\delta}_r = \boldsymbol{\delta}(\boldsymbol{\theta}_r)$ . A single realization from this  $K$ -dimensional multivariate normal distribution can be generated using conditional cumulative distribution function (CDF) inversion and a point  $\mathbf{u} = \{u_k\}_{k=1}^K \in [0, 1]^K$ . We obtain the first component  $\hat{\delta}_{r,1}^{(c)}$  as the  $u_1$ -quantile of the sampling distribution of  $\hat{\delta}_1^{(c)} \mid \boldsymbol{\theta}_r$ . For the remaining components, we generate  $\hat{\delta}_{r,k}^{(c)}$  as the  $u_k$ -quantile of the sampling distribution of  $\hat{\delta}_k^{(c)} \mid \{\hat{\delta}_s^{(c)} = \hat{\delta}_{r,s}^{(c)}\}_{s=1}^{k-1}, \boldsymbol{\theta}_r$ .

Implementing this process with a pseudorandom sequence of  $m$  points  $\{\mathbf{u}_r\}_{r=1}^m \in [0, 1]^K$  simulates a sample from the approximate sampling distribution of  $\hat{\boldsymbol{\delta}}^{(c)}$  according to  $\Psi$ . We substitute this sample  $\{\hat{\boldsymbol{\delta}}_r^{(c)}\}_{r=1}^m$  into the posterior approximation in (6) to yield samples of posterior probabilities. For each scalar estimand in  $\boldsymbol{\delta}(\boldsymbol{\theta})$ , we first consider the probability

$$\tau_{\boldsymbol{\delta},r,k}^{(c)} = \Phi\left(\frac{\delta_k - \hat{\delta}_{r,k}^{(c)}}{\sqrt{c^{-1}\Lambda_{k,k}(\boldsymbol{\theta}_r)}}\right), \quad (7)$$

where  $\boldsymbol{\delta}$  is a general vector of  $K$  interval endpoints and  $\Phi(\cdot)$  is the standard normal CDF. We approximate the probability in the  $k^{\text{th}}$  row of (2) as  $\tau_{H_1,r,k}^{(c)} = \tau_{\delta_{U,r,k}}^{(c)} - \tau_{\delta_{L,r,k}}^{(c)}$ . The collection of  $\{\tau_{H_1,r,k}^{(c)}\}_{k=1}^K$  values corresponding to  $\{\mathbf{u}_r\}_{r=1}^m$  and  $\{\boldsymbol{\theta}_r\}_{r=1}^m \sim \Psi$  define our proxy to the joint sampling distribution of  $\boldsymbol{\tau}(\mathcal{D}_c)$ . We acknowledge that this proxy to the sampling distribution of posterior probabilities relies on asymptotic results, and it may differ materially from the true sampling distribution of  $\boldsymbol{\tau}(\mathcal{D}_c)$  for finite  $c$ .

The proxy sampling distribution therefore only motivates our theoretical result in Theorem 1. This result guarantees that the logit of  $\tau_{H_1,r,k}^{(c)}$  is an approximately linear function of  $c$  for all scalar estimands in  $\boldsymbol{\delta}(\boldsymbol{\theta})$ . We later adapt this result to assess the operating characteristics of a trial across a broad range of sample sizes by estimating the true sampling distribution of  $\boldsymbol{\tau}(\mathcal{D}_c)$  at only *two* values of  $c$ . Each  $\tau_{H_1,r,k}^{(c)}$  value depends on the value for  $\hat{\boldsymbol{\delta}}_r^{(c)}$ , which depends on the sample size  $c$ , the parameter value  $\boldsymbol{\theta}_r$ , and the point  $\mathbf{u}_r$ . In Theorem 1, we fix both  $\boldsymbol{\theta}_r$  and  $\mathbf{u}_r$  to explore the behaviour of  $\tau_{H_1,r,k}^{(c)}$  as a deterministic function of  $c$ .

**Theorem 1.** *For any  $\boldsymbol{\theta}_r \sim \Psi$ , let the conditions for Lemma 1 be satisfied. Define  $\text{logit}(x) = \log(x) - \log(1-x)$ . We consider a given point  $\mathbf{u}_r \in [0, 1]^K$  and distributions for  $\mathbf{X}$ ,  $\mathbf{W}$ , and the cluster size  $n_j$ . For  $k = 1, \dots, K$ , the functions  $\tau_{\delta_{r,k}}^{(c)}$  in (7) are such that*

(a)  $\tau_{\delta_{r,k}}^{(c)} \approx \Phi(a_k(\delta_k, \boldsymbol{\theta}_r)\sqrt{c} + b_k(\mathbf{u}_r))$  for large  $c$ , where  $a_k(\delta_k, \boldsymbol{\theta}_r) = (\delta_k - \delta_{r,k})/\sqrt{\Lambda_{k,k}(\boldsymbol{\theta}_r)}$  and  $b_k(\cdot)$  are functions that do not depend on  $c$ .

(b)  $\lim_{c \rightarrow \infty} \frac{d}{dc} \text{logit}[\tau_{\delta_{U,r,k}}^{(c)} - \tau_{\delta_{L,r,k}}^{(c)}] = (0.5 - \mathbb{I}\{\delta_{r,k} \notin (\delta_{L,k}, \delta_{U,k})\}) \min\{a_k(\delta_{U,k}, \boldsymbol{\theta}_r)^2, a_k(\delta_{L,k}, \boldsymbol{\theta}_r)^2\}$ .

We prove parts (a) and (b) of Theorem 1 in Web Appendices A.2 and A.3. Hagar and Stevens (2025) considered a similar theoretical result that did not accommodate dependent data nor account for marginal or multiple estimands. The methods proposed in this paper therefore accommodate a broader set of data-driven comparisons in Bayesian trials. We now discuss the practical implications of Theorem 1. The limiting derivative in part (b) is a constant that does not depend on  $c$ . For each marginal probability in the joint proxy sampling distribution, the linear approximation to  $l_{H_1,r,k}^{(c)} = \text{logit}(\tau_{H_1,r,k}^{(c)})$  as a function of  $c$  is thus a good global approximation for large sample sizes. This linear approximation should be locally suitable for a range of smaller sample sizes. Therefore, the quantiles of the sampling distribution of  $l_{H_1,r,k}^{(c)}$  change linearly as a function of  $c$  when  $\boldsymbol{\theta}_r$  is held constant across simulation repetitions. In Section 3, we exploit and adapt this linear trend in the proxy sampling distribution to flexibly model the logits of  $\boldsymbol{\tau}(\mathcal{D}_c)$  as linear functions of  $c$  when independently simulating samples  $\mathcal{D}_{c,r}$  according to  $\boldsymbol{\theta}_r \sim \Psi$ . While the proxy sampling distribution is predicated on asymptotic results, we illustrate the good performance of our SSD procedure with finite sample sizes  $c$  in Section 4.



### 3 Sample Size Determination Procedure

We generalize the results from Theorem 1 to develop a procedure for Bayesian SSD that can easily be implemented when estimating posterior probabilities by simulating data  $\mathcal{D}_c$ . This procedure is described in Algorithm 1. It performs well for moderate and large sample sizes, and we estimate the sampling distribution of  $\boldsymbol{\tau}(\mathcal{D}_c)$  at *only* two values of  $c$ :  $c_0$  and  $c_1$ . This initial sample size  $c_0$  can be selected based on the anticipated budget for the trial. In Algorithm 1, we add a subscript to  $\mathcal{D}_{c,r}$  to distinguish whether the data are generated according to the model  $\Psi_0$  or  $\Psi_1$  defined in Section 2.1. That is,  $\mathcal{D}_{c_0,r}$  and  $\mathcal{D}_{c_1,r}$  represent data generated according to  $\Psi_0$  and  $\Psi_1$ , respectively. The subscript on the number of clusters  $c$  is not related to the hypothesis.

In addition to the choices discussed in Section 2, we specify a distribution for the  $n_j \times K$  matrix of responses  $\mathbf{Y}_j$  at the cluster level, denoted broadly by  $p(\mathbf{Y}_j; \boldsymbol{\theta})$ . We must also specify parameters to generate the cluster sizes  $\{n_j\}_{j=1}^c$ , covariates  $\mathbf{X}_{N \times p}$ , and latent effects  $\mathbf{W}_{c \times Kq}$ . We collectively denote these parameters as  $\boldsymbol{\zeta}$ . To implement Algorithm 1, we define criteria for the probabilities of making the correct and incorrect decisions in the trial. Under  $\Psi_1$  where  $H_1$  is true, we want  $\mathbb{E}_{\Psi_1}[Pr(\nu(\mathcal{D}_c) = 1 \mid \boldsymbol{\theta})] \geq \Gamma_1$ . We want  $\mathbb{E}_{\Psi_0}[Pr(\nu(\mathcal{D}_c) = 1 \mid \boldsymbol{\theta})] \leq \Gamma_0$  under  $\Psi_0$  where  $H_0$  is true. Algorithm 1 details a general application of our methodology, and we later describe potential modifications.

---

**Algorithm 1** Procedure to Determine the Number of Clusters

---

- 1: **procedure** CLUSTERSSD( $p(\mathbf{Y}_j; \boldsymbol{\theta})$ ,  $\boldsymbol{\delta}(\cdot)$ ,  $\boldsymbol{\delta}_L$ ,  $\boldsymbol{\delta}_U$ ,  $p(\boldsymbol{\theta})$ ,  $\Psi_0$ ,  $\Psi_1$ ,  $m$ ,  $c_0$ ,  $\boldsymbol{\zeta}$ ,  $\Gamma_0$ ,  $\Gamma_1$ )
  - 2:   Compute  $\{\boldsymbol{\tau}(\mathcal{D}_{c_0,0,r})\}_{r=1}^m$  obtained with  $\boldsymbol{\theta}_r \sim \Psi_0$ .
  - 3:   Choose  $\boldsymbol{\gamma}$  to ensure  $m^{-1} \sum_{r=1}^m \mathbb{I}\{\nu(\mathcal{D}_{c_0,0,r}) = 1\} \leq \Gamma_0$ .
  - 4:   Compute  $\{\boldsymbol{\tau}(\mathcal{D}_{c_0,1,r})\}_{r=1}^m$  obtained with  $\boldsymbol{\theta}_r \sim \Psi_1$ .
  - 5:   If  $m^{-1} \sum_{r=1}^m \mathbb{I}\{\nu(\mathcal{D}_{c_0,1,r}) = 1\} \geq \Gamma_1$ , choose  $c_1 < c_0$ . If not, choose  $c_1 > c_0$ .
  - 6:   Compute  $\{\boldsymbol{\tau}(\mathcal{D}_{c_1,1,r})\}_{r=1}^m$  obtained with  $\boldsymbol{\theta}_r \sim \Psi_1$ .
  - 7:   **for**  $k$  in  $1:K$  **do**
  - 8:     Sort logits  $\{l_k(\mathcal{D}_{c_0,1,r})\}_{r=1}^m$  and  $\{l_k(\mathcal{D}_{c_1,1,r})\}_{r=1}^m$  and pair their corresponding order statistics with linear approximations to obtain  $m \hat{l}_k(\mathcal{D}_{c,1})$  estimates for new  $c$  values.
  - 9:   Obtain  $\{\hat{\boldsymbol{\tau}}(\mathcal{D}_{c,1,r})\}_{r=1}^m$  as the inverse logits of the estimates  $\{\hat{l}_k(\mathcal{D}_{c,1})\}_{k=1}^K$  whose linear approximations were defined using  $\{\boldsymbol{\tau}_k(\mathcal{D}_{c_0,1,r})\}_{k=1}^K$ .
  - 10:   Find  $c_2$ , the smallest  $c \in \mathbb{Z}^+$  such that  $m^{-1} \sum_{r=1}^m \mathbb{I}\{\hat{\nu}(\mathcal{D}_{c,1,r}) = 1\} \geq \Gamma_1$ .
  - 11:   **return**  $c_2$  as recommended  $c$
- 

We now elaborate on several steps of Algorithm 1. In Line 3, we choose a suitable vector of thresholds  $\boldsymbol{\gamma}$  to ensure the estimate for  $\mathbb{E}_{\Psi_0}[Pr(\nu(\mathcal{D}_c) = 1 \mid \boldsymbol{\theta})]$  based on the formula in (4) is at most  $\Gamma_0$ . There are many combinations of the individual thresholds  $\{\gamma_k\}_{k=1}^K$  that will attain the desired bound for  $\mathbb{E}_{\Psi_0}[Pr(\nu(\mathcal{D}_c) = 1 \mid \boldsymbol{\theta})]$ . Without loss of generality, we assume that the estimands in  $\boldsymbol{\delta}(\boldsymbol{\theta})$  are indexed according to their importance (i.e., the first scalar estimand corresponds to the most important outcome). We recommend obtaining the vector  $\boldsymbol{\gamma}$  by sequentially choosing  $\gamma_k$  from  $k = 1$  to  $K$  to satisfy criteria for the individual comparisons between  $\tau_k(\mathcal{D}_c)$  and  $\gamma_k$ . We illustrate this procedure for an example in Section 4.

We emphasize that all posterior probabilities approximated in Lines 2 to 6 of Algorithm 1 are obtained

by simulating data according to  $\Psi_0$  or  $\Psi_1$ . Lines 7 and 8 compute logits of these probabilities under  $\Psi_1$ :  $l_k(\mathcal{D}_{c,1,r}) = \text{logit}(\tau_k(\mathcal{D}_{c,1,r}))$ , where the subscript  $k$  corresponds to the individual estimand. We therefore recommend calculating posterior probabilities using a nonparametric kernel density estimate of the posterior distribution so that these logits are finite. We construct linear approximations separately for each estimand using these logits in Line 8. We use these linear approximations to estimate logits of posterior probabilities for new values of  $c$  as  $\hat{l}_k(\mathcal{D}_{c,1})$ . We place a hat over the  $l$  here to convey that this logit was estimated using a linear approximation instead of a sample with  $c$  clusters. This notation also removes the subscript  $r$  since the linear approximations are not created based on samples  $\mathcal{D}_{c_0,1,r}$  and  $\mathcal{D}_{c_1,1,r}$  that share the same index  $r$ .

Given the linear trend in the proxy sampling distribution quantiles discussed in Section 2.3, it is reasonable to construct these linear approximations based on order statistics of estimates of the true sampling distributions when the value of the individual estimand  $\delta_{r,k}$  is similar for all  $\theta_r \sim \Psi_1$ . When  $\Psi_1$  is nondegenerate, the process in Line 8 can be modified. We instead split the logits of the posterior probabilities for each  $c$  value into subgroups based on the order statistics of their  $\delta_{r,k}$  values before constructing the linear approximations. Our linear approximations concern the individual estimands in  $\delta(\theta)$ ; however, we must account for the dependence between the individual estimands in the joint sampling distribution of  $\tau(\mathcal{D}_c)$  when considering new values of  $c$ . We do so by grouping the estimated logits  $\hat{l}_k(\mathcal{D}_{c,1})$  across estimands based on the sample  $\mathcal{D}_{c_0,1,r}$  that defined their linear approximation. In Line 10, we find the smallest value of  $c$  such that our estimate for  $\mathbb{E}_{\Psi_1}[Pr(\nu(\mathcal{D}_c) = 1 \mid \theta)]$  based on the indicators  $\{\hat{\nu}(\mathcal{D}_{c,1,r})\}_{r=1}^m$  that correspond to  $\{\hat{\tau}(\mathcal{D}_{c,1,r})\}_{r=1}^m$  is at least  $\Gamma_1$ .

We did not estimate the sampling distribution of  $\tau(\mathcal{D}_{c_1})$  under  $\Psi_0$  in Algorithm 1. In Section 4, we consider models  $\Psi_0$  that assign all weight to  $\theta_r$  values such that  $\delta_k(\theta_r)$  equals  $\delta_{L,k}$  or  $\delta_{U,k}$  for all  $k = 1, \dots, K$ . For such models  $\Psi_0$ , large-sample results (Bernardo and Smith, 2009; Golchi and Willard, 2024) guarantee that the probability of making the incorrect decision for a particular set of thresholds  $\gamma$  is roughly constant across a range of large  $c$  values. If using a more general model  $\Psi_0$ , Algorithm 1 can be adapted to implement the process in Lines 6 to 9 under  $\Psi_0$  to efficiently estimate the sampling distribution of  $\tau(\mathcal{D}_c)$  for new values of  $c$ . These estimated sampling distributions could be used to choose an optimal set of thresholds  $\gamma$  for each sample size  $c$  considered.

Lastly, we quantify the impact of simulation variability on the sample size recommendation by constructing bootstrap confidence intervals for the optimal sample size. We construct these confidence intervals by sampling  $m$  times with replacement from  $\{\tau(\mathcal{D}_{c_0,1,r})\}_{r=1}^m$  and  $\{\tau(\mathcal{D}_{c_1,1,r})\}_{r=1}^m$  obtained in Algorithm 1. We note that posterior probabilities for each of the  $K$  individual estimands are resampled jointly. We obtain a new sample size recommendation by implementing the process in Lines 7 to 10 of Algorithm 1 with the *bootstrap* estimates of the sampling distributions at  $c_0$  and  $c_1$ . This process is repeated  $M$  times, and a bootstrap confidence interval for the optimal  $c$  is calculated using the percentile method (Efron, 1982). The

width of this confidence interval can help inform the choice for the number of simulation repetitions  $m$ .

Bootstrap confidence intervals for the design operating characteristics at a given value of  $c$  can similarly be constructed. For each of the  $M$  sets of bootstrap samples, the linear approximations obtained using the process in Lines 7 to 8 of Algorithm 1 give rise to a new estimate of the operating characteristics. A bootstrap confidence interval for the operating characteristic can also be calculated using the percentile method. In Section 4, we consider the performance of Algorithm 1 and construct bootstrap confidence intervals for an example motivated by a current clinical trial.

## 4 Application to the SSTaRLeT Trial

We will apply our proposed approach to the Shorter and Safer Treatment Regimens for Latent Tuberculosis (SSTaRLeT) trial (Menzies, 2024). This trial uses an adaptive platform non-inferiority design where decision criteria are specified with respect to three binary endpoints. The goal of the trial is to establish non-inferiority of two new tuberculosis preventive medications with respect to the reference treatment in terms of safety. Safety is defined using the primary outcome of a grade 3 to 5 adverse event (AE) and two secondary outcomes, completion of the treatment by patients as well as non-tolerability defined as occurrence of a set of reactionary symptoms. To showcase the utility of the proposed approach, we will focus on one interim analysis and a pairwise comparison between one of the new treatments and the reference treatment. However, we emphasize that our approach can be generalized to accommodate the more complex design. Additionally, several design parameter choices have been adjusted from those used for SSTaRLeT, meaning the conclusions in this section are not directly applicable to the real trial.

The trial considers  $K = 3$  estimands based on the binary endpoints. The first estimand  $\delta_1(\boldsymbol{\theta})$  is the difference in the marginal probabilities of experiencing an AE between the new ( $A = 1$ ) and reference ( $A = 0$ ) treatment arms. Estimands  $\delta_2(\boldsymbol{\theta})$  and  $\delta_3(\boldsymbol{\theta})$  are respectively the differences between marginal probabilities of non-completion and non-tolerability in the new and reference treatments. For estimands  $k = 1$  to 3, the trial subhypotheses are defined as follows:

$$H_{0,k} : \delta_k(\boldsymbol{\theta}) \geq \delta_{U,k} \text{ vs. } H_{1,k} : \delta_k(\boldsymbol{\theta}) < \delta_{U,k},$$

where  $\delta_{U,k}$  is the non-inferiority margin for subhypothesis  $k$ . The non-inferiority margins for this trial are  $\delta_{U,1} = 0.04$  and  $\delta_{U,2} = \delta_{U,3} = 0.1$ . Thus, large positive differences between probabilities of experiencing an AE, non-completion, and non-tolerability are associated with inferiority.

The interim decision criteria are defined based on evidence of inferiority with respect to any of the three outcomes. Specifically, the experimental treatment arm will be dropped if sufficient evidence points to inferiority in AE safety, completion, or tolerability. That is, the treatment arm will be dropped if for any  $k = 1, 2, 3$ ,

$$\tau_k(\mathcal{D}_c) = Pr(\delta_k(\boldsymbol{\theta}) < \delta_{U,k} \mid \mathcal{D}_c) \leq \gamma_k.$$

The decision thresholds  $\gamma_k$  are specified to bound the probability of making an incorrect non-inferiority decision (i.e., incorrectly continuing with an inferior treatment) by  $\Gamma_0$ . Our goal, therefore, is to determine the interim sample size  $c$  required to achieve a desired probability  $\Gamma_1$  of correct non-inferiority (i.e., correctly continuing with a non-inferior treatment).

SSTaRLeT is a cluster randomized trial where households are randomized into either of the treatment arms with outcome-adjusted allocation ratios. However, since adjustments are scheduled at interim analyses and we focus on the first interim analysis, the outcome-adaptive randomization scheme is not incorporated in our simulations.

We consider four design scenarios for this trial that are summarized in Table 1. The first three scenarios correspond to non-inferiority under  $H_1$  and the fourth corresponds to inferiority under  $H_0$ . We aim to select a sample size  $c$  such that the probability of correctly continuing the acceptable treatment in scenario 2 is at least  $\Gamma_1 = 0.85$ . The decision thresholds  $\gamma$  will be selected to bound the probability of incorrectly continuing the unacceptable treatment in scenario 4 by  $\Gamma_0 = 0.08$ . The probabilities of concluding non-inferiority in scenarios 1 (clearly acceptable) and 3 (barely acceptable) are considered for sensitivity analysis.

Table 1: Marginal probabilities for binary outcomes in various design scenarios

Arm	Reference	Experimental Treatment			
		1: Clearly Acceptable	2: Acceptable	3: Barely Acceptable	4: Unacceptable
AE rate	2%	2%	3%	5%	6%
Completion rate	75%	75%	72%	70%	65%
Non-tolerability rate	25%	25%	28%	30%	35%

We now broadly overview the data that inform the posterior of  $\delta(\theta)$ . We generate a matrix of outcomes  $\mathbf{Y}_{N \times 3}$ , where each row corresponds to a patient. The  $k^{\text{th}}$  column of  $\mathbf{Y}_{N \times 3}$  corresponds to the  $k^{\text{th}}$  binary outcome: the occurrence of an AE, non-completion, or non-tolerability. There are no additional observed covariates  $\mathbf{X}_{N \times p}$  for this example. As such,  $\mathcal{D}_c = \{\mathbf{Y}_{N \times 3}, \mathbf{A}_N\}$ . Furthermore, we use three intraclass correlation coefficient (ICC) settings – low, moderate, and high – to explore various levels of dependence between the binary outcomes. Since we marginalize over cluster-specific latent effects, the ICC settings materially impact sample size recommendations. It is therefore important to efficiently consider various ICC settings in trial design. We thoroughly describe the data generation procedure for all described settings in Web Appendix C, and direct readers to [Golchi et al. \(2022\)](#) for additional context.

Each outcome is analyzed using a separate Bayesian logistic regression model with random intercepts:

$$y_{k,j,i} \sim \text{BIN}(1, \text{expit}(\eta_{k,j,i})), \quad \text{where } \eta_{k,j,i} = \beta_{0,k} + \beta_{1,k}A_{j,i} + w_{k,j}, \quad (8)$$

For the model in (8), the subscripts are such that  $k$  indexes the estimand,  $j$  indexes the cluster, and  $i$  indexes the observation within the  $j^{\text{th}}$  cluster. In the model corresponding to the  $k^{\text{th}}$  estimand,  $\beta_{0,k}$  and  $\beta_{1,k}$  represent a common intercept and slope and  $w_{k,j} \sim \mathcal{N}(0, \sigma_k^2)$  are cluster-specific intercepts. The latent effects

for this example are  $\mathbf{W}_{c \times 3}$ , where the  $k^{\text{th}}$  column contains the random intercepts for the  $k^{\text{th}}$  estimand. The parameters  $\boldsymbol{\theta}$  consist of the  $3 \times 1$  vectors of coefficients  $\beta_0$  and  $\beta_1$  along with the variances for the random intercepts  $\{\sigma_k^2\}_{k=1}^3$ . We use diffuse priors for all parameters as described in Web Appendix C.

We first present the simulation results for the low ICC setting. When implementing Algorithm 1 with  $m = 10^4$  simulation repetitions, an initial sample size of  $c_0 = 120$  was selected based on an anticipated budget for the trial. The probability model  $\Psi_0$  for this example corresponds to scenario 4 in Table 1. Based on the estimated sampling distribution obtained in Line 2 of Algorithm 1, a threshold of  $\gamma_1 = 0.8$  corresponding to the primary outcome was selected in Line 3. Equal thresholds  $\gamma_2 = \gamma_3 = 0.54$  were then chosen for the secondary outcomes to bound the probability of incorrect non-inferiority by  $\Gamma_0 = 0.08$ .

The probability model  $\Psi_1$  for this example corresponds to scenario 2 in Table 1. Given this choice for  $\Psi_1$ , the probability of correct non-inferiority at  $c_0 = 120$  was estimated as 0.7813, which is less than the target probability of  $\Gamma_1 = 0.85$ . A larger sample size of  $c_1 = 170$  was explored in Line 6 of Algorithm 1. The linear approximations in Lines 7 and 8 were constructed using  $c_0 = 120$  and  $c_1 = 170$ . We note that the probability models  $\Psi_0$  and  $\Psi_1$  for this example do not incorporate uncertainty in the parameter values used to generate the data. These choices for  $\Psi_0$  and  $\Psi_1$  mirror those used to design SSTaRLeT, but our methodology accommodates nondegenerate models  $\Psi_0$  and  $\Psi_1$  as described in Section 3. Based on the linear approximations in Algorithm 1, the recommended sample size in Line 10 for the low ICC setting is  $c_2 = 152$ . A 95% bootstrap confidence interval for the optimal sample size obtained using the procedure detailed in Section 3 with  $M = 10^4$  bootstrap samples is [149, 155].

Figure 1 visualizes the probability of continuing the experimental treatment for each scenario in Table 1 with respect to  $c$  for the low ICC setting. This probability corresponds to correct non-inferiority for scenarios 1, 2, and 3 and incorrect non-inferiority for scenario 4. The black curves were estimated using linear approximations to logits of posterior probabilities at only two sample sizes ( $c_0 = 120$  and  $c_1 = 170$ ) using the process in Lines 4 to 9 of Algorithm 1. The dashed curves represent pointwise 95% bootstrap confidence intervals for the design operating characteristics obtained using linear approximations with bootstrap samples as described in Section 3. The blue curves were simulated by independently generating samples of data to estimate sampling distributions of posterior probabilities at  $c = \{100, 110, \dots, 200\}$  for each setting.

Although the blue curves are impacted by simulation variability, we use them as surrogates for the true design operating characteristics. We observe good alignment for all four scenarios between the black curves estimated using linear approximations and the blue ones obtained by independently simulating samples. Furthermore, the blue curves are generally contained within the pointwise 95% bootstrap confidence intervals for the range of sample sizes we consider. However, the black curves are substantially easier to obtain since we need only estimate sampling distributions of posterior probabilities at two values of  $c$ . Even so, it took roughly 40 minutes on a high-computing server to estimate each black curve in Figure 1 when approximating

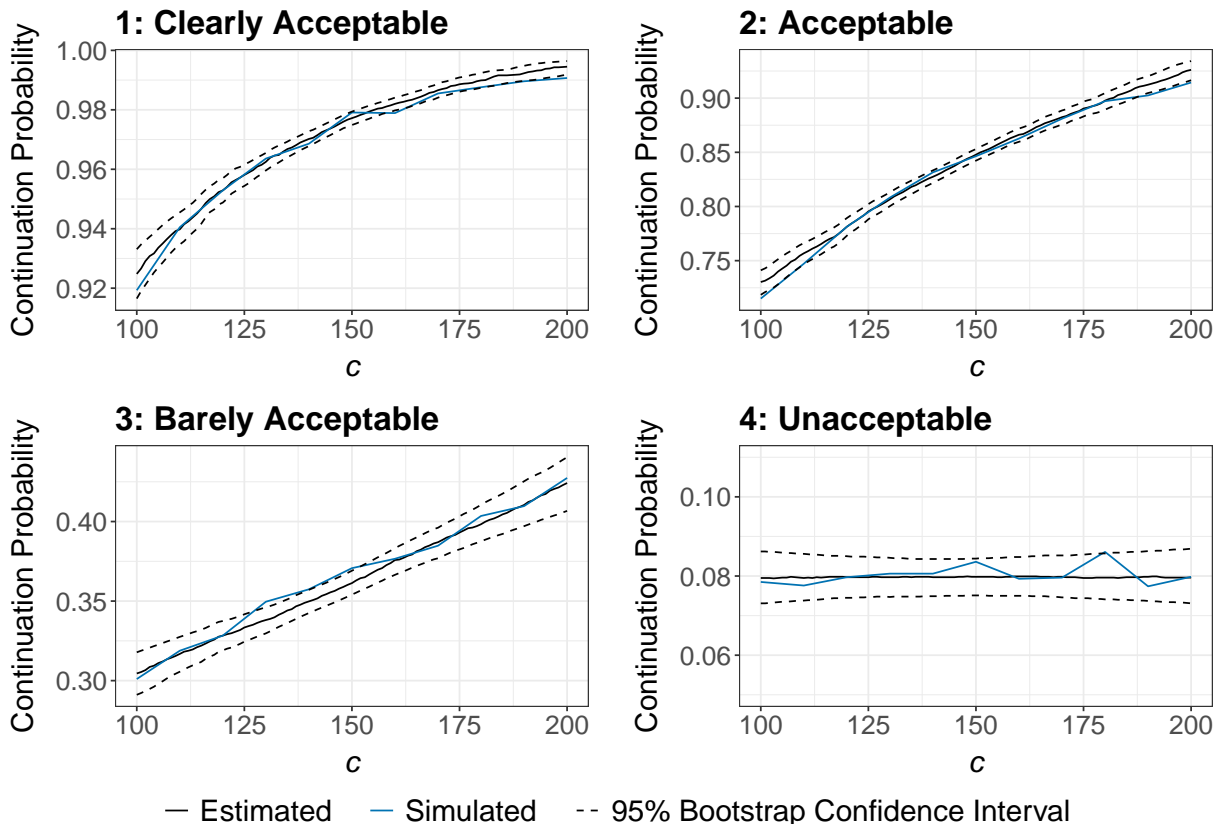


Figure 1: The probability of continuing the new treatment for the low ICC setting. The black curves are estimated using linear approximations. The dashed curves are pointwise 95% bootstrap confidence intervals. The blue curves arise from simulating sampling distributions for many  $c$  values.

each posterior using Markov chain Monte Carlo with only one chain of 500 burnin iterations and 1500 retained draws. We considered 11 values of  $c$  to simulate each blue curve in Figure 1, taking roughly 4 hours using the same computing resources. Unlike standard methods, our approach also allows practitioners to assess design operating characteristics for new values of  $c$  without conducting additional simulations.

To facilitate comparison with the low ICC setting, we repeated the process described above with the same decision thresholds  $\gamma = (0.8, 0.54, 0.54)$  for the moderate and high ICC settings. Figures 2 and 3 respectively visualize the continuation probabilities for the moderate and high ICC settings. We again observe good alignment between the black curves estimated using our method and the blue ones obtained by traditional simulation. The computational savings associated with using our methodology are similar for all ICC settings.

Our method recommended a sample size of  $c = 169$  for the moderate ICC setting; the 95% bootstrap confidence interval for the optimal sample size was  $[166, 175]$ . The corresponding sample size recommendation and confidence interval for the high ICC setting were  $c = 186$  and  $[180, 193]$ . These results demonstrate that sample size recommendations are sensitive to the ICC settings when we marginalize over the distributions of the latent effects. Thus, it is crucial to explore various ICC settings during trial design, which increases the

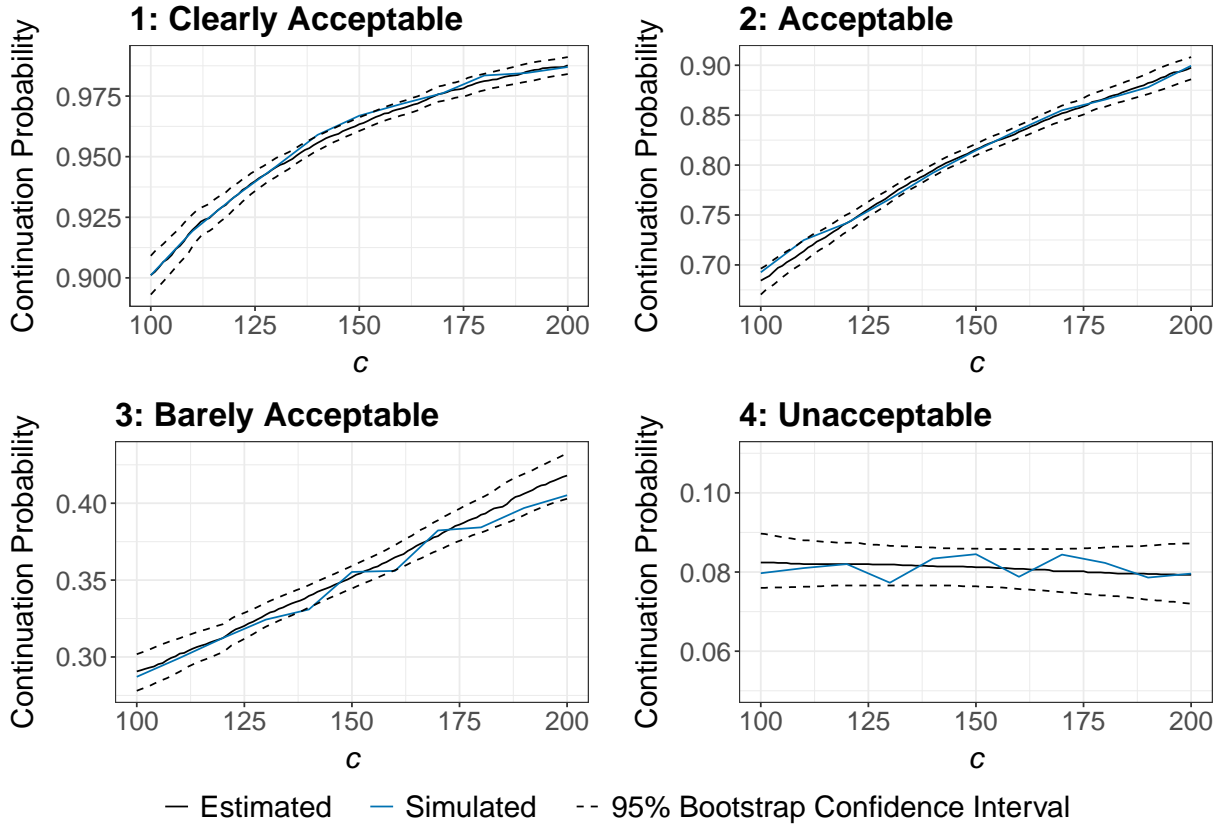


Figure 2: The probability of continuing the new treatment for the moderate ICC setting. The black curves are estimated using linear approximations. The dashed curves are pointwise 95% bootstrap confidence intervals. The blue curves arise from simulating sampling distributions for many  $c$  values.

number of design configurations considered. Our methodology facilitates the efficient assessment of operating characteristics for each configuration.

## 5 Discussion

In this paper, we proposed an efficient framework to assess design operating characteristics for Bayesian clinical trials with clustered data. This framework determines the minimum number of clusters required to ensure the probability of making a correct decision is sufficiently large while bounding the probability of making an incorrect decision. The computational efficiency of our framework is motivated by considering a proxy for the joint sampling distribution of posterior probabilities across multiple estimands. We use the behaviour in this large-sample proxy distribution to justify estimating true sampling distributions at only two sample sizes. Our method therefore drastically reduces the number of simulation repetitions required to design Bayesian trials. Furthermore, we repurpose our estimates of the sampling distribution to construct bootstrap confidence intervals that quantify the impact of simulation variability on the sample size recommendation. Our methodology can be broadly used in clinical settings where large-sample regularity conditions are satisfied – including settings with a single estimand or those that do not require

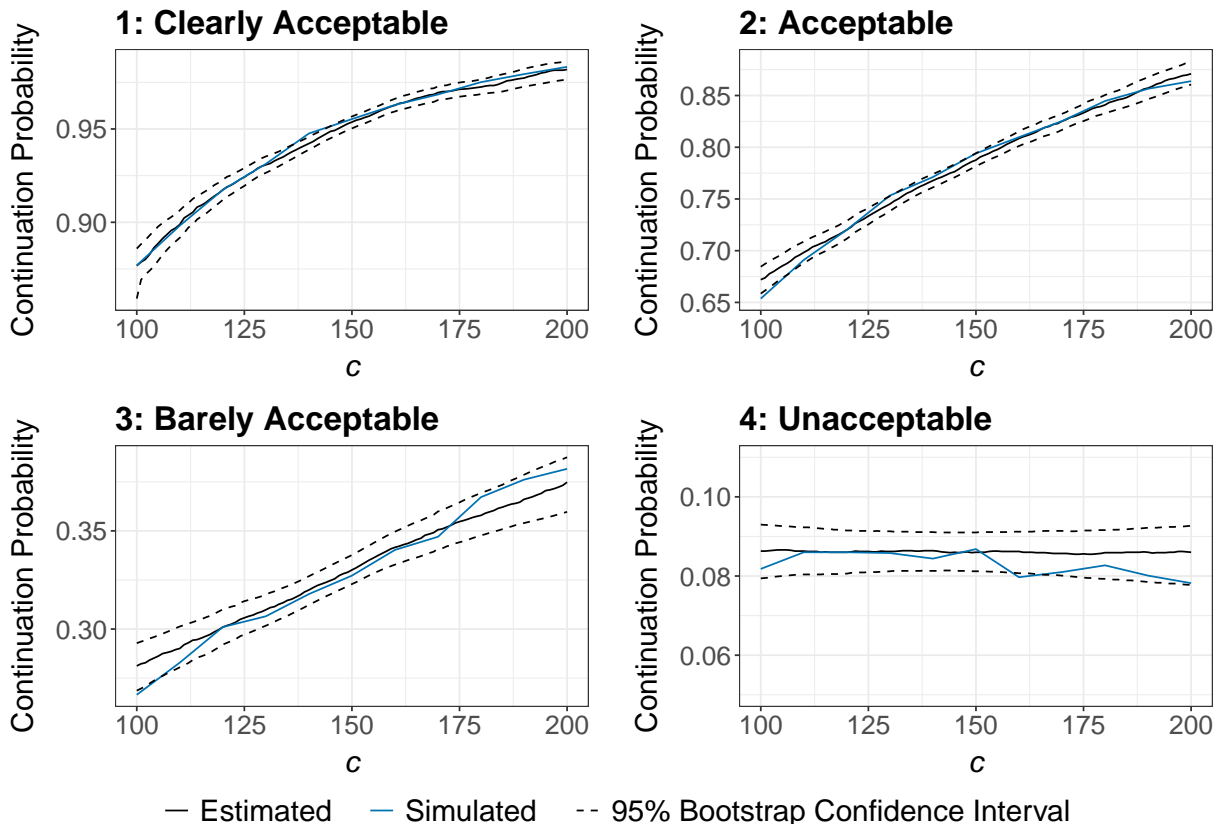


Figure 3: The probability of continuing the new treatment for the high ICC setting. The black curves are estimated using linear approximations. The dashed curves are pointwise 95% bootstrap confidence intervals. The blue curves arise from simulating sampling distributions for many  $c$  values.

marginalization via Bayesian G-computation.

Our motivating example in Section 4 provides insight for future research. First, our example reflects that clinicians often want to consider the trial operating characteristics for various data generation processes  $\Psi_1$  and  $\Psi_0$ . We already efficiently explore the sample size space, but analogs to Theorem 1 that enable efficient consideration of the  $\Psi_1$ -space and  $\Psi_0$ -space for a given sample size would also be useful. Moreover, we analyzed the data in our simulated trials using separate models for each binary outcome. This choice was made for simplicity, but it would be worthwhile to develop Bayesian models for analyzing dependent binary outcomes that do not compromise the computational feasibility of trial design. When multiple outcomes inform complex decision criteria in clinical trials, it is also important to propose more sophisticated procedures to choose decision thresholds than the ad-hoc methods used in this paper. These extensions could help control design operating characteristics in settings where some but not all of the subhypotheses  $\{H_{0,k}\}_{k=1}^K$  are true.

The methods proposed in this paper can be extended to accommodate more complex designs, such as group sequential designs that allow for early stopping. We note that the theoretical foundation for our proxy distribution is applicable in sequential settings. However, we must take care when extending our procedure



from Section 3 to ensure linear approximations are constructed in such a way that maintains the proper level of dependence in the joint sampling distribution of posterior probabilities across interim analyses. Since this extension is not trivial, we plan to address sequential settings in future work.

Lastly, the use of dynamic borrowing methods to incorporate information from prior trials has become increasingly common. Depending on the borrowing method used, the conditions for the BvM theorem may not be satisfied. Further research is needed to clarify when these conditions are met and develop extensions for scenarios where the conditions are not satisfied.

## Supplementary Material

The Web Appendices referenced in the paper are available in an online supplement. The code to conduct the numerical studies in the paper is available online: <https://github.com/lmhagar/ClusterDOCs>.

## Acknowledgements

The authors would like to thank Dr. Dick Menzies for his comments and suggestions regarding the SSTaRLeT application component of this article.

## Funding

Luke Hagar acknowledges the support of a postdoctoral fellowship from the Natural Sciences and Engineering Research Council of Canada (NSERC). Shirin Golchi acknowledges support from NSERC, Canadian Institute for Statistical Sciences (CANSSI), and Fonds de recherche du Québec - Santé (FRQS).

## References

- Bernardo, J. M. and A. F. Smith (2009). *Bayesian Theory*, Volume 405. John Wiley & Sons.
- Berry, S. M., B. P. Carlin, J. J. Lee, and P. Muller (2010). *Bayesian adaptive methods for clinical trials*. CRC press.
- Bretz, F., W. Maurer, W. Brannath, and M. Posch (2009). A graphical approach to sequentially rejective multiple test procedures. *Statistics in Medicine* 28(4), 586–604.
- Daniel, R., J. Zhang, and D. Farewell (2021). Making apples from oranges: comparing noncollapsible effect estimators and their standard errors after adjustment for different covariate sets. *Biometrical Journal* 63(3), 528–557.
- De Santis, F. (2007). Using historical data for Bayesian sample size determination. *Journal of the Royal Statistical Society: Series A (Statistics in Society)* 170(1), 95–113.

- Dmitrienko, A., A. C. Tamhane, and B. L. Wiens (2008). General multistage gatekeeping procedures. *Biometrical Journal* 50(5), 667–677.
- Efron, B. (1982). *The Jackknife, the Bootstrap and Other Resampling Plans*. SIAM.
- FDA (2019). Adaptive designs for clinical trials of drugs and biologics — Guidance for industry. Center for Drug Evaluation and Research, U.S. Food and Drug Administration, Rockville, MD.
- FDA (2022). Multiple endpoints in clinical trials - Guidance for industry. Center for Drug Evaluation and Research, U.S. Food and Drug Administration, Rockville, MD.
- Golchi, S. (2022). Estimating design operating characteristics in Bayesian adaptive clinical trials. *Canadian Journal of Statistics* 50(2), 417–436.
- Golchi, S. and J. J. Willard (2024). Estimating the sampling distribution of posterior decision summaries in Bayesian clinical trials. *Biometrical Journal* 66(8), e70002.
- Golchi, S., J. J. Willard, E. Pullenayegum, D. G. Bassani, L. G. Pell, K. Thorlund, and D. E. Roth (2022). A Bayesian adaptive design for clinical trials of rare efficacy outcomes with multiple definitions. *Clinical Trials* 19(6), 613–622.
- Gubbiotti, S. and F. De Santis (2011). A Bayesian method for the choice of the sample size in equivalence trials. *Australian & New Zealand Journal of Statistics* 53(4), 443–460.
- Hagar, L. and N. T. Stevens (2024). Fast power curve approximation for posterior analyses. *Bayesian Analysis*, 1 – 26 doi.org/10.1214/24-BA1469.
- Hagar, L. and N. T. Stevens (2025). An economical approach to design posterior analyses. *arXiv preprint arXiv:2411.13748*.
- Han, L., A. Arfè, and L. Trippa (2024). Sensitivity analyses of clinical trial designs: Selecting scenarios and summarizing operating characteristics. *The American Statistician* 78(1), 76–87.
- Hemming, K., M. Taljaard, M. Moerbeek, and A. Forbes (2021). Contamination: How much can an individually randomized trial tolerate? *Statistics in Medicine* 40(14), 3329–3351.
- Holm, S. (1979). A simple sequentially rejective multiple test procedure. *Scandinavian journal of statistics*, 65–70.
- Kalton, G. (1968). Standardization: A technique to control for extraneous variables. *Journal of the Royal Statistical Society: Series C (Applied Statistics)* 17(2), 118–136.

- Keil, A. P., E. J. Daza, S. M. Engel, J. P. Buckley, and J. K. Edwards (2018). A Bayesian approach to the g-formula. *Statistical Methods in Medical Research* 27(10), 3183–3204.
- Lehmann, E. L. and G. Casella (1998). *Theory of Point Estimation*. Springer Science & Business Media.
- Menzies, D. (2024). An adaptive trial to find the safest and shortest TB preventive regimens. <https://clinicaltrials.gov/study/NCT06498414>.
- Murray, D. M. (1998). *Design and Analysis of Group-Randomized Trials*, Volume 29. Oxford University Press.
- Neuhaus, J. M., J. D. Kalbfleisch, and W. W. Hauck (1991). A comparison of cluster-specific and population-averaged approaches for analyzing correlated binary data. *International Statistical Review/Revue Internationale de Statistique*, 25–35.
- O’Hagan, A., J. W. Stevens, and M. J. Campbell (2005). Assurance in clinical trial design. *Pharmaceutical Statistics: The Journal of Applied Statistics in the Pharmaceutical Industry* 4(3), 187–201.
- O’Hagan, A. and J. W. Stevens (2001). Bayesian assessment of sample size for clinical trials of cost-effectiveness. *Medical Decision Making* 21(3), 219–230.
- Spiegelhalter, D. J., K. R. Abrams, and J. P. Myles (2004). *Bayesian Approaches to Clinical Trials and Healthcare Evaluation*, Volume 13. John Wiley & Sons.
- Spiegelhalter, D. J., L. S. Freedman, and M. K. Parmar (1994). Bayesian approaches to randomized trials. *Journal of the Royal Statistical Society: Series A (Statistics in Society)* 157(3), 357–387.
- van der Vaart, A. W. (1998). *Asymptotic Statistics*. Cambridge Series in Statistical and Probabilistic Mathematics. Cambridge University Press.
- Wang, F. and A. E. Gelfand (2002). A simulation-based approach to Bayesian sample size determination for performance under a given model and for separating models. *Statistical Science* 17(2), 193–208.
- Willard, J., S. Golchi, and E. E. Moodie (2024). Covariate adjustment in Bayesian adaptive randomized controlled trials. *Statistical Methods in Medical Research* 33(3), 480–497.